AD-A107 333 BROWN UNIV PROVIDENCE RI DEPT OF CHEMISTRY F/G 7/4
VIBRATIONAL SPECTRA OF OXYGEN- AND BORON-ISOTOPICALLY SUBSTITUT--ETC(U)
SEP 81 C F WINDISCH, W M RISEN N00014-75-C-0883
UNCLASSIFIED TR-81-02 NL

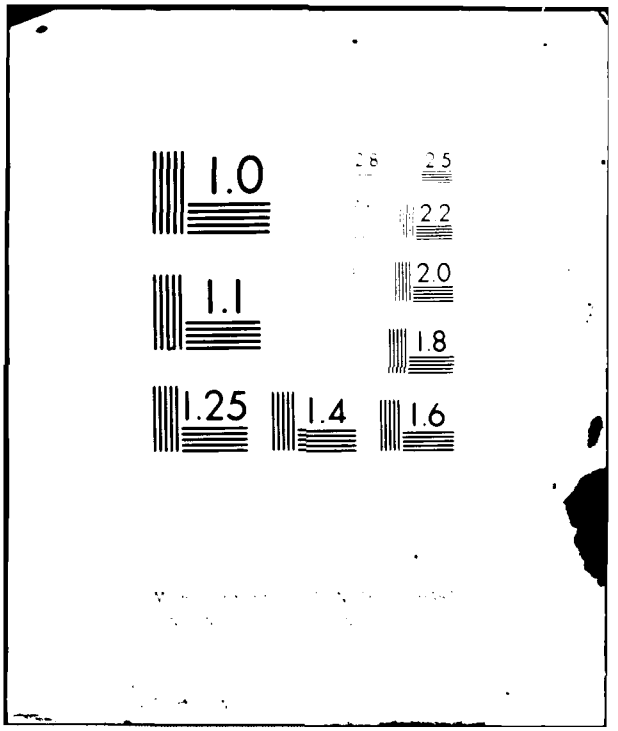
1.0
1.1
1.25
1.4
1.6
1.8
2.0
2.2
2.5

(12)

OFFICE OF NAVAL RESEARCH

Contract ONR-N00014-75-C-0883 NR-051-539

TECHNICAL REPORT NO. TR-81- 02

Vibrational Spectra of Oxygen- and Boron-Isotopically Substituted B_2O_3 Glasses

by

Charles F. Windisch and William M. Risen, Jr.

September 15, 1981

Prepared for Publication

in the

Journal of Non-crystalline Solids

Department of Chemistry
Brown University
Providence, R. I. 02912

September 15, 1981

SECURITY CLASSIFICATION OF THIS PAGE (When Data Entered)

REPORT DOCUMENTATION PAGE

READ INSTRUCTIONS BEFORE COMPLETING FORM

1. REPORT NUMBER: 2 TR-81-02	2. GOVT ACCESSION NO.: AD-A107 333
3. RECIPIENT'S CATALOG NUMBER:	
4. TITLE (and Subtitle): Vibrational Spectra of Oxygen- and Boron-Isotopically Substituted B_2O_3 Glasses	5. TYPE OF REPORT & PERIOD COVERED: Technical
	6. PERFORMING ORG. REPORT NUMBER:
7. AUTHOR(s): Charles F. Windisch and William M. Risen, Jr	8. CONTRACT OR GRANT NUMBER(s): N00014-75-C-0883 NR-051-539
9. PERFORMING ORGANIZATION NAME AND ADDRESS: Department of Chemistry, Brown University, Providence, Rhode Island 02912	10. PROGRAM ELEMENT, PROJECT, TASK AREA & WORK UNIT NUMBERS: 1-413
11. CONTROLLING OFFICE NAME AND ADDRESS: Office of Naval Research, United States Navy	12. REPORT DATE: September 15, 1981
	13. NUMBER OF PAGES: 35
14. MONITORING AGENCY NAME & ADDRESS (if different from Controlling Office)	15. SECURITY CLASS. (of this report)
	15a. DECLASSIFICATION/DOWNGRADING SCHEDULE

16. DISTRIBUTION STATEMENT (of this Report)

Distribution Unlimited; Approved for Public Release

17. DISTRIBUTION STATEMENT (of the abstract entered in Block 20, if different from Report)

18. SUPPLEMENTARY NOTES

19. KEY WORDS (Continue on reverse side if necessary and identify by block number)

glass, Raman spectra, B_2O_3, borate glass, boroxol ring, glass structure, isotopically substituted glasses

20. ABSTRACT (Continue on reverse side if necessary and identify by block number)

The Raman spectra of ^{10}B, ^{11}B, ^{16}O, ^{18}O, and mixed isotopic compositions of B_2O_3 (gl) are reported. The 808 cm^{-1} band assigned to the boroxol ring structure is found to shift upon oxygen isotope substitution, and not to depend on the boron mass. It is replaced by four bands, in the intensity ratio 1:3:3:1, in the case of the 50% ^{16}O-50% ^{18}O-containing material. On the other hand, the frequencies other principal bands depend on the masses of both boron and oxygen. The ca 1260 cm^{-1} band, in particular, depends on the masses of both, and shifts with-

Continue over

DD FORM 1 JAN 73 1473 EDITION OF 1 NOV 65 IS OBSOLETE S/N 0102-014-6601

SECURITY CLASSIFICATION OF THIS PAGE (When Data Entered)

out broadening upon partial oxygen substitution. The analysis of these data shows that both a local unit, behaving as predicted for the boroxol ring, and a continuous random network of connecting bonds are manifested in the spectra.

Vibrational Spectra of Oxygen- and Boron-Isotopically Substituted B_2O_3 Glasses

Charles F. Windisch, Jr. and William M. Risen, Jr.
Metcalf Research Laboratories
Department of Chemistry
Providence, Rhode Island 02912 U.S.A.

Abstract

The Raman spectra of ^{10}B, ^{11}B, ^{16}O, ^{18}O, and mixed isotopic compositions of B_2O_3 (gl) are reported. The 808 cm^{-1} band assigned to the boroxol ring structure is found to shift upon oxygen isotope substitution, and not to depend on the boron mass. It is replaced by four bands, in the intensity ratio 1:3:3:1, in the case of the 50% ^{16}O - 50% ^{18}O-containing material. On the other hand, the frequencies other principal bands depend on the masses of both boron and oxygen. The ca 1260 cm^{-1} band, in particular, depends on the masses of both, and shifts without broadening upon partial oxygen substitution. The analysis of these data shows that both a local unit, behaving as predicted for the boroxol ring, and a continuous random network of connecting bonds are manifested in the spectra.

Introduction

The structure of vitreous B_2O_3 has long been a subject of considerable interest. Following the suggestion of Goubeau and Keller (1), for some time boroxol rings (the B_3O_3 units depicted in Figure 1) have been thought to be major constituents of the structure. This postulate has been supported by the results from a number of studies, especially that of Bray and coworkers (2), who showed that the B- and O-NMR spectra are consistent with boroxol rings being present, and that, in any event, there are two different oxygen sites and boron is in a site of axial symmetry. In addition, Kristiansen and Krogh-Moe (3) and Brill (4) interpreted the vibrational spectrum of B_2O_3 (gl), and Walrafen, et al (5) that of the melt as well, in terms of the boroxol ring as a major structural component. Important support for the postulate w provided by Mozzi and Warren (6), who showed that the X-ray radial distribution function (RDF) is well-fit by a boroxol-based model. Finally, the orientation-dependence of the Raman spectra of B_2O_3 (gl) films recently has been found to support this postulate (7).

On the other hand, crystalline B_2O_3 consists of "condensed $BO_{1.5}$ chains" (connected BO_3 triangles) (8), and Elliott (9) recently concluded that a continuous random network (CRN) of planar BO_3 units, the vitreous analog, best fits the RDF. No evidence for boroxol rings was educed in that study. Nor was any found in the molecular dynamics study of Soules and Varshneya (10). They showed that given a system of classical particles (B and O atoms in the ratio of 2 to 3) interacting under reasonable, spherically symmetric interatomic forces, a B_2O_3 "glass" formed theoretically by very rapidly cooling the system from a random fluid does not contain boroxol rings.

Such support for the CRN approach, and especially its utility

in the interpretation of vibrational spectra of other covalently bound oxide glasses (11,12) led Galeener, Lucovsky and Mikkelsen (13) to employ it to interpret the spectrum of B_2O_3 (g1) and attempt to resolve some of the conflicting structural interpretations. The spectra were analyzed using a nearest neighbor central force network dynamics model. The results showed that if random dihedral angles between connected BO_3 units (which share an oxygen) are assumed, the dominant (808 cm^{-1}) band is not accounted for by the CRN. Ultimately, the conclusion was reached from the narrowness of calculated angular distributions and comparison with the spectrum of $H_3B_3O_6$ that the boroxol ring structure is present.The CRN aspect of the treatment, it was emphasized, is approximate and does not include a number of potentially important force field elements.

Although it is possible to suggest how the import of certain of the conflicting conclusions could be minimized, such as by pointing out the limited theoretical time scale or incompleteness of the potential function of the MD calculations, for example, the disparate results remain. Since the CRN approach is intuitively appealing and has been successful in other inorganic glass systems, it is important to help establish the actual structure in B_2O_3 (g1).

The vibrational spectra of isotopically substituted forms of B_2O_3 (g1) can provide useful information. In the boroxol model the B_3O_3-rings, which are joined through extra-annular B-O-B bonds to other rings, can execute localized vibrations. These are modes in which momentum is conserved without motion of atoms outside of the unit. Isotopic splitting or shifting patterns for such modes are directly calculable on the basis of the dynamics of the unit as a

pseudo-molecule. In the CRN model for B_2O_3 (gl), as for all glasses in which all atoms are bound in a network such that the only identifiable unit smaller than the whole network is that comprised of an atom and it nearest neighbors, the results of isotopic substitution are different in several ways. The more important is that the frequencies of the collective mode should shift, upon partial or complete substitution for a given type of atom, as would be expected for an atom with a mass that is the same as the number-averaged mass of the isotopes present. Moreover, the associated bandwidth (FWHH) should not change. For vibrations of an isolated unit this would not be the case. The other expected result consists of the details predicted for a given model. Thorpe and Galeener (14), for example, derived expressions for the four "band edges" of an idealized A_2X_3 CRN consisting of AX_3 planar triangles and found that two modes should depend on the mass only of X, while the other two depend on the mass only of A.

Isotopic substitution vibrational studies have not been done as frequently on glasses as might be expected. One reason for this is that the synthetic tools for obtaining controlled composition samples in a practical way with limited and expensive isotopes have only recently been reported (15). A more important reason is that the vibrational bands of glasses often are quite broad. Of course it still is possible to obtain isotopically shifted spectra, but,when the shifts are much less than the bandwidth,much of the detailed information contained in spectra of mixed isotope materials is lost or difficult to analyze. Fortunately, the strongest band in the Raman spectrum of B_2O_3 (gl) at 808 cm^{-1} (excluding the "Bose-Einstein" peak at very low frequencies) is very sharp. Its full width at half height (FWHH) is about 15 cm^{-1} and it is sufficiently

separated from other bands that its behavior upon isotopic substitution can be observed unambiguously. This band has been assigned to a mode of the boroxol ring by Krogh-Moe (3) and others. Other Raman bands in B_2O_3 (gl) are less sharp, but some are widely-enough separated that their shifts in fully substituted materials can be observed.

If the 808 cm^{-1} band is due to a boroxol ring vibration there are several possible outcomes from isotopic substitution. One is that the vibration is localized and its frequency depends on the masses of both B and O. If this is the case, the relationships between the magnitudes of the B- and O-displacements in the eigenvector can be determined from the frequency shifts when B- and O-substitutions are done separately. Another is that it is localized but depends only on the mass of either B or O. Given its symmetry (it would have to be one of the totally symmetric modes in D_3h), in this case the complete form of the eigenvector is obtainable. In either of these cases, the spectrum of B_2O_3 (gl) containing two or more isotopes of a given atom would have a predictable form. For example, if half of the oxygens were ^{16}O and half were ^{18}O, four bands having the intensity ratio 1:3:3:1 would be seen. The other general case is the CRN of connected BO_3 triangles. As noted above, if the mode is a coupled one the band should shift according to the average mass of the substituted atom but not change shape or bandwidth.

If the boroxol ring is an important structural element, it is still true that they can be connected randomly. This would be a CRN of boroxol units, and the isotopically substituted material would have a spectrum which contains some bands that behave as if they were due to pseudomolecules (execute local vibrations) and some, due to the connecting links, that would behave in a number-

weighted average mass manner.

The preparation and Raman spectra of various isotopic forms of B_2O_3(gl) and the analysis of the data in terms of the structural issue are reported below.

Experimental

Five different isotopic forms of B_2O_3(gl) were prepared for study of the oxygen- and boron-mass effects. The compounds used as starting materials determined the actual isotopic contents such that those labelled ^{16}O had 100% ^{16}O, while ^{18}O was 99% ^{18}O, ^{11}B was 80.2% ^{11}B, and ^{10}B was 92.4% ^{10}B. Using these specifications, the materials prepared were $^{11}B_2{}^{16}O_3$, $^{11}B_2{}^{18}O_3$, $^{10}B_2{}^{16}O_3$, $^{11}B_4{}^{16}O_2{}^{18}O_2$ (i.e. $^{11}B_2{}^{16}O_3 \cdot {}^{11}B_2{}^{18}O_3$), and $^{10}B_2{}^{11}B_2{}^{16}O_6$ (i.e $^{10}B_2{}^{16}O_3 \cdot {}^{11}B_2{}^{16}O_3$). As an example, taking into account the actual abundances, the empirical formula of $^{11}B_2{}^{16}O_3$ is $^{11}B_{1.6}{}^{10}B_{0.4}{}^{16}O_3$.

Preparation of ^{18}O-labelled B_2O_3(cryst.)

Following the procedure of Abys, et al (15), $^{11}B_2{}^{18}O_3$(cryst) was synthesized by the hydrolysis of $^{11}BCl_3$ with $H_2{}^{18}O$, followed by dehydration of the adid product, according to the reactions

$$^{11}BCl_3 + 3H_2{}^{18}O \xrightarrow{P \lesssim 10^{-3}\ \text{Torr}} B(^{18}OH)_3 + 3HCl(g)$$

$$2B(^{18}OH)_3 \xrightarrow[350^\circ]{P \lesssim 10^{-3}\ \text{Torr}} B_2{}^{18}O_3(s) + 3H_2{}^{18}O(g)$$

The product $H_2{}^{18}O$, which was recovered, was 99% ^{18}O-enriched and obtained from Prochem (Summit, N.J., U.S.A.). The reactions were carried out in a vacuum line and the product stored under dry N_2 when at atmospheric pressure.

Preparation of Glasses

The natural abundance glass, $^{11}B_2{}^{16}O_3$(gl), was prepared by heating reagent grade $H_3{}^{11}B^{16}O_3$ in a Pt crucible at ca 1000°C in an electric furnace for one hour, at which time it was bubble-free. The melt was quenched by allowing it to cool at ambient temperature. The $^{10}B_2{}^{16}O_3$(gl) was prepared in an analogous manner from $H_3{}^{10}B^{16}O_3$ (92.4% ^{10}B). The mixed isotope glass $^{10}B_2{}^{11}B_2{}^{16}O_6$ was prepared analogously from a physical mixture of $H_3{}^{11}B^{16}O_3$ and $H_3{}^{10}B^{16}O_3$.

The oxygen-18 labelled B_2O_3(gl), $^{11}B_2{}^{18}O_3$(gl), was prepared by transferring ca 0.3 g of $^{11}B_2{}^{18}O_3$ (cryst) to a small Pt boat under dry N_2. Also under N_2 the boat was placed in a quartz tube and the tube closed with a fitting containing a closed 3-way stopcock. The assembly was inserted into a cold furnace, as shown in Figure 2, and evacuated. The temperature was raised slowly to 1000°C and held there for one hour. It was then removed, allowed to cool to room temperature, filled with dry N_2, and opened in a dry N_2-filled atmosphere, where the Pt boat was removed. Small pieces of $^{11}B_2{}^{18}O_3$(gl) were removed from the boat and stored over $CaSO_4$ dessicant.

The mixed isotope glass $^{11}B_4{}^{16}O_3{}^{18}O_3$(gl) was prepared in a manner similar to that of the $^{11}B_2{}^{18}O_3$, except that a molar equivalent amount of $^{11}B_2{}^{16}O_3$ (cryst), which had been synthesized in a procedure identical to that for $^{11}B_2{}^{18}O_3$ (cryst), was weighed under N_2 and mixed with $^{11}B_2{}^{18}O_3$(cryst). The mixture was made into a mixed isotope glass using the sealed tube method described above.

The preparative procedures used were designed to minimize two hydrolytic effects. One is simple hydrolysis of the B_2O_3 itself, and the other is $^{16}O/^{18}O$ exchange in the ^{18}O-containing melts.

Sample Handling

Due to the hygroscopic nature of vitreous B_2O_3, certain precautions were taken during sample handling and spectral analysis. Again, this to prevent observation of artifacts in the spectra and to prevent isotopic exchange. To establish conditions for handling, a piece of $^{11}B_2{}^{18}O_3$(gl) was transferred under dry N_2 to the sample cell shown in Figure 3 and the cell maintained with a dry N_2 atmosphere. The Raman spectrum of the sample was measured under these conditions. Then the sample was removed from the cell and exposed to the air. Over the course of 24 hours no significant change was detected in the spectral features associated with the glass, but the appearance of new features, especially a band at 880 cm^{-1}, indicated the formation of a layer of orthoboric acid on the glass surface. These observations helped establish proper conditions for sample handling and detection of hydrolysis.

Raman Spectra

Laser Raman spectra were measured using a Jarrell-Ash 25-300 Spectrometer with a Spectra Physics 164 Argon ion laser. Typically the 488.0 nm line of the laser was employed, along with a narrow band interference filter, and, as required, polarization scrambler between the sample and entrance slit of the spectrometer. Experiments were done in the 90^{o} scattering geometry.

Results

The Raman spectrum of $^{11}B_2{}^{16}O_3$(gl) in the 1550-35 cm^{-1} region is shown in Figure 4 for the HH and HV polarizations. The frequencies and FWHH values for two of the strongest bands in the region are noted. This spectrum agrees well with those reported previously (3,5,13).

As is well known, the dominant ratio for the broader 1260 cm^{-1} band is ca 0.7.

The Raman spectra of $^{11}B_2{}^{16}O_3$(gl), $^{10}B_2{}^{16}O_3$(gl), and $^{11}B_2{}^{18}O_3$(gl) are shown in Figure 5, curves (a), (b), and (c). The shift of each feature is noted to emphasize its dependence on mass. Comparison of curves (a) and (b) in Figure 5 shows the effect of changing the boron mass, while that of curve (a) with curve (c) shows the oxygen mass-dependence. It is clear that there are important modes, including the 808 cm^{-1} band, which depend almost entirely on the mass of oxygen. The bands whose frequencies depend on both masses are labelled X, while those labelled O depend significantly only on the mass of oxygen. The frequencies of the bands and their shifts are listed in Table 1.

As seen in Table 1 and Figure 6(a), complete ^{18}O-labelling causes the 808 cm^{-1} band to shift by -48 cm^{-1} to 760 cm^{-1}. This shift occurs without broadening of the band. On the other hand, substitution of ^{10}B for ^{11}B causes no shift in the 808 cm^{-1} band, as shown in Figure 6(c). The vibrational mode at 808 cm^{-1} involves motion of the oxygens only, at least to a good approximation.

The effect of isotopic substitution on the 1260 cm^{-1} band is shown in Figures 7(a) and 7(c). The frequency clearly depends on the masses of both B and O. The FWHH of this band remains 35±1 cm^{-1}, although this is clearer in the case of complete ^{18}O-^{16}O substitution than it is in the case of the ^{11}B-^{10}B substitution. Other bands in this region are broader, as is characteristic of bands for glasses generally, and, analogously to the 1260 cm^{-1} band, shift upon

substitution of either boron or oxygen.

The spectra of mixed isotope materials is particularly revealing in the regions of these two well-defined features. As shown in Figure 6(b), the band at 808 cm^{-1} in $^{11}B_2{}^{16}O_3$(gl) is replaced by a composite of four bands in $^{11}B_4{}^{16}O_3{}^{18}O_3$(gl). These features, having the apparent intensity relationship 1:3:3:1, appear at 808, 791, 777, and 760 cm^{-1} respectively. Since no boron motion is involved, the mixed boron isotope materials band remains at 808 cm^{-1}, as shown in Figure 6(d).

The behavior of the 1260 cm^{-1} band for $^{11}B_2{}^{16}O_3$(gl) is quite different. As shown in Figure 7(b), the position of this band in $^{11}B_4{}^{16}O_3{}^{18}O_3$(gl) is 1243 cm^{-1}. It has nearly the same shape and bandwidth as it does when it appears in the spectrum of $^{11}B_2{}^{16}O_3$(gl) at 1260 cm^{-1}. When the glass $^{11}B_2{}^{10}B_2{}^{16}O_6$(gl) is measured, the band is observed at 1272 cm^{-1}, midway between its positions in the spectra of $^{10}B_2{}^{16}O_3$(gl) and $^{11}B_2{}^{16}O_3$(gl). Again the band shape and FWHH values (35 cm^{-1}) are essentially unchanged as the atomic masses are varied.

Finally, the depolarization ratios at the positions of several bands, taken approximately without extensive deconvolution of the several effects contributing to scattering, are plotted versus frequency in Figure 8. This "depolarization spectrum" in the terms of Kobliska and Solin (16), is not useful presently where there are no bands, so those points are replaced by dashed lines. This plot and the other results are discussed below.

Discussion

The fact that the 808 cm^{-1} band shifts on oxygen-mass change but not on boron mass change within experimental error, shows that

the mode involves essentially only oxygen motion. The fact that it is replaced by four bands, one at 808 cm^{-1}, in the ratio 1:3:3:1 instead of by one band in $^{11}B_4{}^{16}O_3{}^{18}O_3$ is strong evidence that the mode is a highly localized one. Indeed, the observation of such a splitting pattern appears to be unprecedented for vitreous materials.

On the other hand, the behavior of the 1260 cm^{-1} band is not characteristic of a localized mode. If it were such a mode, it would split into discrete bands or broaden to envelope several shifted but overlapped bands. It does neither. The breadth, nearness of neighboring bands, and relatively low intensity of each of the other bands makes their analysis subject to the uncertainties of deconvolution and significant baseline correction. This and the fact that the two different types of behavior are exhibitied by the two distinctive bands at 808 and 1260 cm^{-1} make it most useful to focus on their behavior.

Since the types of results expected for both localized and CRN behavior are found experimentally, an appropriate model must provide for a structure in which both can occur. In this context, it is clear that a structure of boroxol rings that are randomly connected through extraannular oxygen atoms is quite suitable. This will be treated in more detail below.

It is useful to consider whether these new spectral results could be interpreted in terms of a CRN of planar BO_3 units. The 1260 cm^{-1} mode (and its shifts) can be rationalized in CRN terms, either as discussed below in the context of the connected boroxol model or as assigned by Mikkelsen and Galeener (13). Except for the 808 cm^{-1} band, the other spectral features could be accounted for in the broad CRN context. The isotopic splitting pattern of the

808 cm^{-1} band is the key to solving the problem, but it must be considered carefully. If either a BO_3 or B_3O_3 (boroxol) ring were vibrationally uncoupled, a symmetric mode (A_1' in D_{3h}) would be Raman active and give rise to four bands in the 1:3:3:1 intensity ratio at the 50% ^{16}O/50% ^{18}O composition. As shown below, this occurs simply for the boroxol ring in which it is possible for the three in-ring oxygens to move without significant coupling of the mode to network motions. However, for BO_3 "triangles" a very special type of mode would have to exist in order for the oxygens to do essentially all the motion and yet for the mode to act as if it were localized. Clearly it is impossible for it actually to be uncoupled from the rest of the network if the "triangles" are joined through the moving oxygens. What may be possible is for each BO_3 to execute the symmetric stretch exactly out-of-phase with the adjacent ones in such a way as to make them appear to be independent. In order for them to do so, some special connecting geometry appears to be required for conservation of both linear and angular momentum. In any event, it seems clear from the CRN studies reported to date that (a) the effect of changing the oxygen mass would have to be an average one if the O-B-O angle is taken as 120°, and (b) the 808 cm^{-1} band remains unaccounted for. The question of the criteria for the formation of special structures within the CRN context is under study.

The presence of localized vibrational behavior has been proposed in other glass systems. Most cases have involved defect structures, but Locovsky (17) and Martin (18) have used local models to explain the spectra of As_2S_3, As_2Se_3, and amorphous chalcogens. For the former two, AsX_3 and As-X-As units were used, and the vibrational frequencies were calculated in good agreement with the data using a scaling

process. Tauc (19), DeFonzo (20), and Finkman, et al (21) reported further analyses of As_2S_3 and As_2Se_3. They showed that by comparing the Raman spectra of the crystalline and amorphous materials, slight k-dependent modes can be identified and associated with isolated molecular vibrations. DeFonzo and Tauc (19) showed that in a glass these modes contribute most to the spectrum. The boroxol ring postulate does not involve defect structures. Rather, the ring is taken to be a major component of the network which, at certain frequencies, can vibrate rather independently of the network.

Further evidence for localized vibrational behavior was reported by Kobliska and Solin (16), who suggested that the more "molecular" the character of an amorphous solid is, the more irregular is its depolarization "spectrum". For example, quite drastic "dips" in ρ are observed in As_2S_3(gl) (16), while amorphous Si, which is thought not to have identifiable pseudo-molecular structures, has an essentially constant value of ρ through the spectrum. The depolarization "spectrum" of B_2O_3(gl), displayed in Figure 8, shows the "irregularity" thus attributable to localized vibrations. This is consistent with our conclusions from the isotopic data.

Since the behavior of the 808 cm^{-1} band supports a local (boroxol) model, but the behavior of the 1260 cm^{-1} band is closer to what is expected for a CRN-mode, it was decided to perform a vibrational analysis of the local models to examine the eigenvectors. Thus, normal coordinate analyses were done on the B_3O_3 ring and BO_3 triangle structure.

Vibrational Analysis

The structures analyzed are shown in Figure 9. The pseudo

atoms X were linearly bonded to each peripheral oxygen and the force field and eigenvectors relevant to each O-X bond were used to monitor the effect of coupling the internal modes of each structure to the network. Variation of the portions of the force field applicable to the O-X bonding should have essentially no effect on the frequency of an uncoupled mode.

The Schachtschneider program (22), based on the Wilson G-F matrix method, was used for the analysis. The symmetry properties, geometry, and masses were incorporated straightforwardly, as done by Krogh-Moe (3). However, the force field was established differently. Reasonable valence force constants were estimated for each structure on the basis of previous work on this and related systems (3,23,24). However, the force field was subjected to such constraints as that the magnitude of the interaction force constants (off-diagonal elements of the field) could not exceed approximately 0.2 of the related bond (diagonal element) constants. While the initial force field was varied a bit to provide a reasonable fit to the observed frequencies, no attempt was made to obtain an exact fit because the goodness-of-fit is not as useful a criterion for a vibrational calculation as is that applied here when knowledge of the vibrational frequencies is not over-complete. In any event, the magnitudes of some of the principal diagonal elements are similar to those of Krogh-Moe (3).

The normal coordinate problem was solved for the isolated B_3O_3 ring and BO_3 triangle first. Then, non-zero values for the force constants relevant to the B-O-X bonds (f_X, O-X stretch; f_θ, B-O-X bend; and $f_{X,R}$, the B-O,O-X stretching interaction) were introduced and varied to determine their effect. The eigenvectors and frequencies computed for the principal A_1 modes of the isolated

boroxol ring (Boroxol(isol.)) and the boroxol ring with attached pseudo atoms X (labeled Boroxol) are given in Figure 10. Also presented there are results for the BO_3X_3 unit.

From these calculations it is clear that only ν_3 of the boroxol ring is independent of the masses of the peripheral atoms and the force field associated with extraannular bonding. Its frequency and form are not changed by varying the mass or force constants due to such bonding, which constitutes the "network bonding". However, other modes of the ring couple with the environment to varying extents; that is, they participate in network-type vibrations. In particular, ν_2 in the 1250-1300 cm^{-1} region and ν_1, in the 1500 cm^{-1} region, involve primarily extraannular bond distention even though ring atoms move considerably. Furthermore, essentially all of the atomic motion in ν_3 is due to oxygen atoms, while ν_1, ν_2, and ν_4 involve motion of both O and B. Naturally, each of the modes of BO_3X_3, including those shown in Figure 10, depends strongly on the O-X bonding.

Further calculations were performed on all of the ^{18}O and ^{10}B isotopic systems studied experimentally. For the boroxol ring structure, substitution of ring atoms only (ν_3 is essentially independent of the extraannular masses) yielded the results shown in Figure 11. The value of ν_3 is calculated to shift from 808 cm^{-1} for $B_3{}^{16}O_3$ to 762 cm^{-1} for $B_3{}^{18}O_3$, and for the C_{2v} species $B_3{}^{18}O{}^{16}O_2$ and $B_3{}^{18}O_2{}^{16}O$ to 793 and 777 cm^{-1} respectively. These are in agreement with their observed positions, as shown below. These frequencies are calculated to be the same with either ^{10}B or ^{11}B, as observed. The other main A_1 modes shift upon substitution of either B or O as shown in Table 2.

Although the comparison of calculated and observed frequencies for ν_3 in Figure 10, and the preceding assignments of the bands are consistent with the interpretation of the mode as a localized one with isotopic splitting, to complete the analysis it is necessary to show that the observed band shape agrees with that calculated. Accordingly, four Lorentzian bands at the calculated positions,with the FWHH of the 808 cm^{-1} band, and in the intensity ratio 1:3:3:1 were added. The individual bands and their sum are shown in Figure 12. The sum band shape is essentially the same as that observed.

Spectroscopically the 1260 cm^{-1} band exhibits network-type behavior upon isotopic substitution. This is evident from the spectra in Figures 7a and 7b for mixed oxygen isotope glasses, in which the band appears at an "average" frequency (± 3 cm^{-1}) between those of the ^{16}O and ^{18}O-labelled glasses. It does not split or broaden. When an "average" oxygen mass of 17 amu is used in the boroxol ring calculations an average frequency between that calculated for completely ^{16}O and ^{18}O substituted rings is obtained for ν_2. Mikkelsen and Galeener (13) assigned this band to a network (TO) mode.

Yet other evidence seems to suggest that the 1260 cm^{-1} band is connected with the vibration of the boroxol ring. Krogh-Moe (3) assigned this band to the A_1 vibration ν_2 (Figure 10) or ν_1 for the "isolated ring", which presumably would involve more network contribution than ν_3. This coupling, it was argued, would cause a breakdown of selection rules and make the band infrared active, as it is, as well as contribute to band broadening.

However, our isotopic results and calculations show that this

band is not primarily associated with the boroxol ring, but represents the participation of ring atoms and extraannular atoms in the network vibrations. Its mass dependence is on both B and O. Moreover, if this mode were essentially a localized ring vibration, it should have resulted in either a splitting or at least a broadening of the band with partial isotopic substitution. Thus, the $B_3O_3^{-3}$ ion in crystalline metaborates (25) has a band at 1600 cm^{-1} which splits predictably with partial ^{10}B substitution. The 1260 cm^{-1} band does not split or broaden.

Our conclusion is that the 1260 cm^{-1} band is best assigned to a delocalized B-O stretch involving both ring and network contributions.

Conclusions

The results for ^{18}O and ^{10}B isotopic substitution in the vitreous B_2O_3 (g1) demonstrate that there is both highly localized vibrational motion characteristic of boroxol rings and network motion characteristic of such rings randomly connected in a network.

Acknowledgments

This work was supported in part by the Office of Naval Research. The authors are grateful for this and for the use of the facilities and support of the Materials Research Laboratory of Brown University sponsored by the Materials Research Laboratory Program of the National Science Foundation. It is a pleasure to acknowledge the helpful advice and discussion with Professor P.J. Bray and his students at Brown, Drs. J. Mikkelsen and F. Galeener of the Xerox Laboratories, Palo Alto, CA, and of George Ogar and Stratos Kamitsos of the Chemistry Department at Brown.

References

1. J. Goubeau and H. Keller, Z. anorg. allg. chem. 272, 303 (1953).
2. G. E. Jellison, Jr., L. W. Panek, P. J. Bray and G. B. Rouse, Jr., J. Chem. Phys. 66, 802 (1977).
3. L. A. Kristiansen and J. Krogh-Moe, Phys. Chem. Glasses 9, 96 (1968).
4. T. W. Bril, Philips Res. Repts. Suppl. No. 2 (1976).
5. G. E. Walrafen, S. R. Samanta and P. N. Krishnan, J. Chem. Phys. 72, 113 (1980).
6. R. L. Mozzi and Warren, J. Appl. Crystallogr. 3, 251 (1970).
7. C. Windisch and W. M. Risen, Jr., submitted to J.N.C.S. (1981)
8. G. E. Gurr, P. W. Montgomery, C. D. Knudson and B. T. Gorres, Acta Cryst. B26, 906 (1970).
9. S. R. Elliott, Phil. Mag. B37, 435 (1978).
10. T. F. Soules and A. K. Varshneya, J. Am. Ceram. Soc. 64, 145 (1981).
11. F. L. Galeener, Phys. Rev. B19, 4292 (1979).
12. F. L. Galeener and J. C. Mikkelsen, Jr., Solid State Commun. 30, 505 (1979).
13. F. L. Galeener, G. Lucovsky and J. C. Mikkelsen, Jr., Phys. Rev. B22, 3983 (1980).
14. M. F.Thorpe and F. L. Galeener, Phys. Rev. B22, 3078 (1980).
15. J. A. Abys, D. M. Barnes, S. Feller, G. Rouse and W. M. Risen, Jr., Mat. Res. Bull. 15, 1581 (1980).
16. R. J. Kobliska and S. A. Solin, Phys. Rev. B8, 756 (1973).
17. G. Lucovsky, Phys. Rev. B6, 1480 (1972).
18. R. M. Martin, Proc. Roy. Soc. A 260, 139 (1961)
19. J. Tauc, "Infrared and Raman Spectroscopy of Amorphous Semiconductors", in Physics of Structurally Disordered Solids, S. S. Mitra (Editor), Plenum Press, New York, 1976, pp 525-540.

20. A. P. DeFonzo, Optic Vibrations in Amorphous and Crystalline As_2S_3 and As_2Se_3, Ph.D. Thesis, Brown University, 1975.

21. E. Finkman, A. P. DeFonzo and J. Tauc, in Proc. of 12th Intl. Conference on Physics of Semiconductors, Teubner, 1974.

22. J. H. Schachtschneider, Techn. Rep. No. 231-64 (Vol. I and II), Shell Development Company, Emeryville, CA (1966).

23. C. Pistorius, J. Chem. Physics 31, 1454 (1959).

24. L. A. Kristiansen, R. W. Mooney, S. J. Cyvin, and J. Brunvoll, Acta Chem. Scand. 19, 1749 (1965).

25. J. P. Bronswijk, The Physics of Non-Crystalline Solids, Fourth International Conference, Clausthal-Zellerfeld, G. H. Frischat (Editor), Trans Tech Publications, 1976, pp 101-107.

Table 1

Raman Frequencies and Shifts for ^{10}B, ^{11}B, ^{16}O, ^{18}O-B_2O_3 Glasses

$\Delta\nu(^{16}O \rightarrow ^{18}O)$ cm^{-1}	$\nu(^{11}B_2{}^{18}O_3(gl)$ cm^{-1}	$\nu(^{11}B_2{}^{16}O_3(gl)$ cm^{-1}	$\nu(^{10}B_2{}^{16}O_3(gl)$ cm^{-1}	$\Delta\nu(^{11}B \rightarrow ^{10}B)$ cm^{-1}
-15	1445	1460	1509	+49
- 9	1320	1329	1373	+44
-25	1235	1260	1284	+24
-32	1176	1208	1238	+30
-48	760	808	808	0
		732	760	+28
- 4	657	661	679	+18
-35	570	605	606	+ 1
-28	472	500	500	0
-25	445	470	472	+ 2
-25	390	415	415	0

Table 2

Calculated Spectral Shifts for A_1' modes of the Boroxol Ring (cm^{-1})

Freq.	$\nu(^{16}O,^{11}B)$	$\nu(^{18}O)$	$\Delta\nu(^{16}O\ ^{18}O)$	$\nu(^{10}B)$	$\Delta\nu(^{11}B\ ^{10}B)$
ν_1	1503	1476	-27	1506	+ 3
ν_2	1283	1279	- 4	1334	+51
ν_3	808	762	-46	808	0
ν_4	490	471	-19	492	+ 2

Figure Captions

1. Representation of the boroxol (B_3O_3 ring structure). The three extraannular oxygens are bound to trigonal planar B atoms and are the only atoms bound to the ring. The dotted lines from these oxygens to the rest of the network are drawn to emphasize that the extra-annular dihedral angles and those angles with vertices at those oxygens are not defined by the model.

2. Vacuum tube (quartz) furnace used in the preparation of ^{18}O-labeled glasses. The three-way stopcock permitted heating of the sample under vacuum and quenching in dry N_2.

3. Plexiglass sample cell used to take Raman spectra of hygroscopic ^{18}O-labeled glasses. Thin glass cover slides served as entrance and exit ports for the laser beam. The sample was inserted on a wire through a side port while under N_2 atmosphere, a cap retaining the seal when the chamber was removed from N_2. Dry N_2 was passed through the chamber between two septums, as noted in the figure, as the spectrum was taken.

4. The 350-1550 cm^{-1} region of the Raman spectrum of $^{11}B_2\ ^{16}O_3$ (gl). The spectrum is shown for two polarization conditions: ———, HV; ----, HH. The frequencies and bandwidths at half-height (FWHH) of the two principal bands are noted.

5. The 350-1550 cm^{-1} region of the Raman spectrum of B_2O_3 (gl) under different types of isotopic substitution; (a) $^{11}B_2\ ^{16}O_3$ (gl)

(b) $^{10}B_2\ ^{16}O_3$ (gl), (c) $^{11}B_2\ ^{18}O_3$ (gl). The symbol X connects those bands whose frequency depends about equally on both the masses of boron and oxygen; the symbol O connects those bands whose frequency depends principally on the mass of oxygen.

6. The Raman spectrum in the vicinity of 800 cm^{-1} of B_2O_3 (gl) for different types and amounts of isotopic substitution. (a) Spectra are shown for both $^{11}B_2\ ^{16}O_3$ (gl) and $^{11}B_2\ ^{18}O_3$ (gl); (b) Spectrum of $^{11}B_4\ ^{16}O_3\ ^{18}O_3$ (gl); (c) Spectra are shown for both $^{11}B_2\ ^{16}O_3$ (gl) and $^{10}B_2\ ^{16}O_3$ (gl); (d) Spectrum of $^{10}B_2\ ^{11}B_2\ ^{16}O_6$ (gl).

7. The Raman spectrum in the vicinity of 1250 cm^{-1} of B_2O_3 (gl) for different types and amounts of isotopic substitution. (a) spectra are shown for both $^{11}B_2\ ^{16}O_3$ (gl) and $^{11}B_2\ ^{18}O_3$ (gl); (b) spectrum of $^{11}B_4\ ^{16}O_3\ ^{18}O_3$ (gl); (c) spectra are shown for both $^{11}B_2\ ^{16}O_3$ (gl) and $^{10}B_2\ ^{16}O_3$ (gl); (d) spectrum of $^{10}B_2\ ^{11}B_2\ ^{16}O_6$(gl).

8. "Depolarization spectrum" for $^{11}B_2\ ^{16}O_3$ (gl). Since readings are not useful in regions where there are no bands, those points are replaced with dashed lines. Ratios were taken approximately, at the peak frequencies of several bands without extensive deconvolution of the several effects contributing to scattering.

9. Geometry and numbering scheme used for both structures in the normal coordinate analyses. Both structures are of D_{3h} symmetry as drawn. Masses (in amu) were taken as follows: ^{10}B, 10.013; ^{11}B, 11.009; ^{16}O, 15.999; ^{18}O, 17.999; X, 5.0.

10. Frequencies and eigenvectors of totally symmetric modes (A_1') calculated for the boroxol ring, the isolated boroxol ring with f_X, f_θ and f_{XR} set equal to zero (isol.), and the BO_3X_3 unit.

11. Comparison of the observed frequencies in the Raman spectrum of $^{11}B_4\ ^{16}O_3\ ^{18}O_3$ (g1), and the calculated frequencies for ν_3 under different degrees of ^{18}O-substitution within the boroxol ring. Expected intensity of each band is given by statistics for substitution in a 50% ^{16}O/50%^{18}O system and is denoted "Rel. comp.".

12. The four Lorentzian bands constructed with appropriate relative amplitudes (1:3:3:1) at each of the calculated frequencies for ν_3, and their sum. The result is an excellent simulation of the observed Raman spectrum of $^{11}B_4\ ^{16}O_3\ ^{18}O_3$ (g1) within this region.

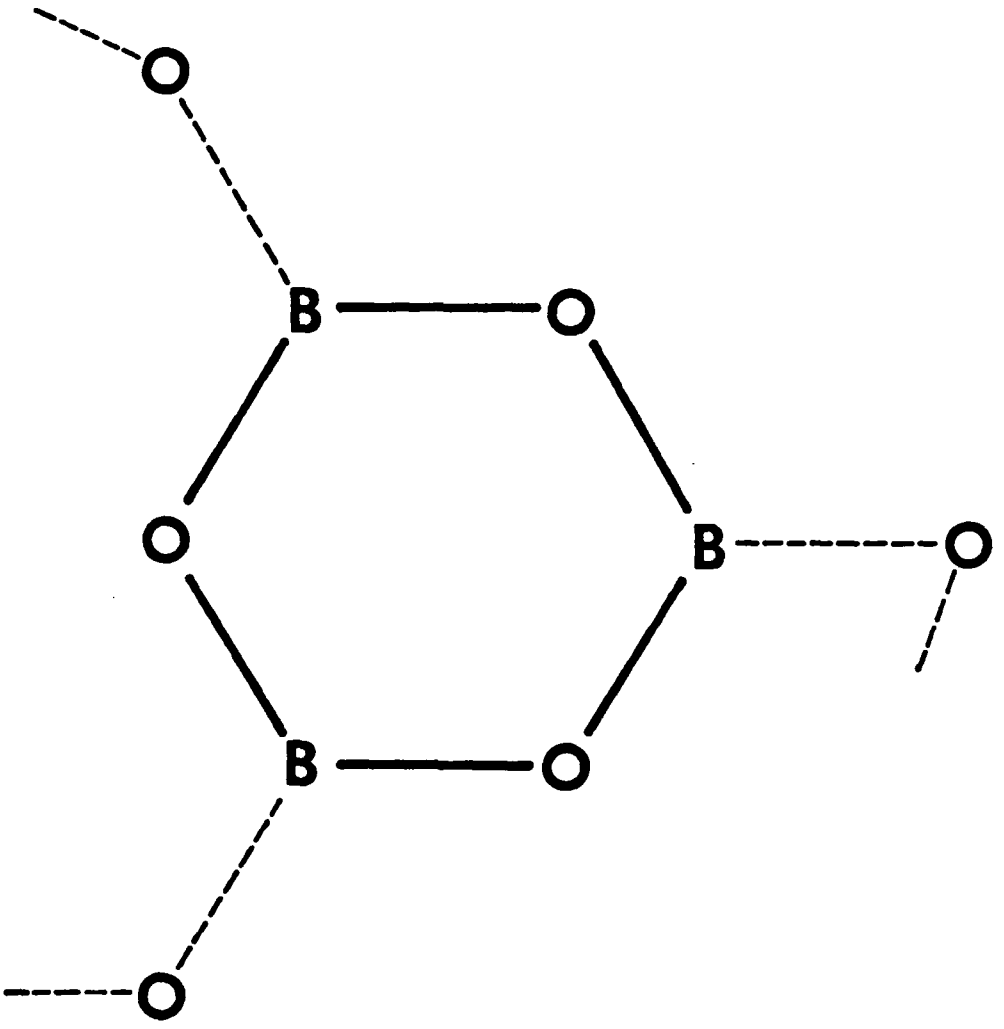
O
B
O
O
B
O
B
O
O

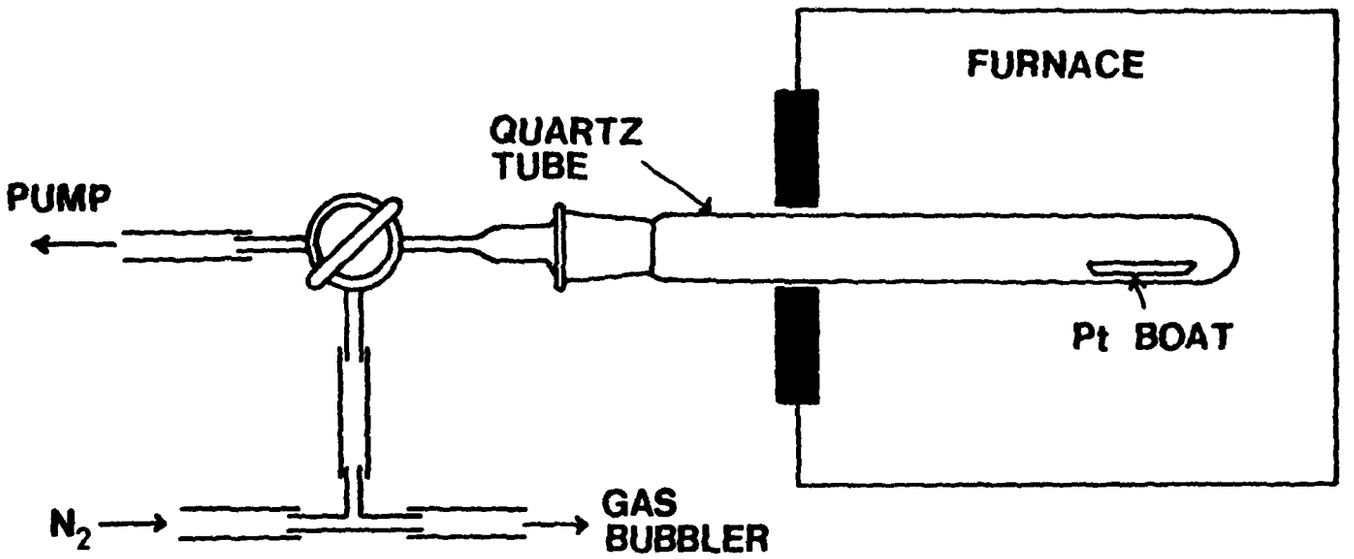
FURNACE
QUARTZ
TUBE
PUMP
Pt BOAT
N_2
GAS
BUBBLER

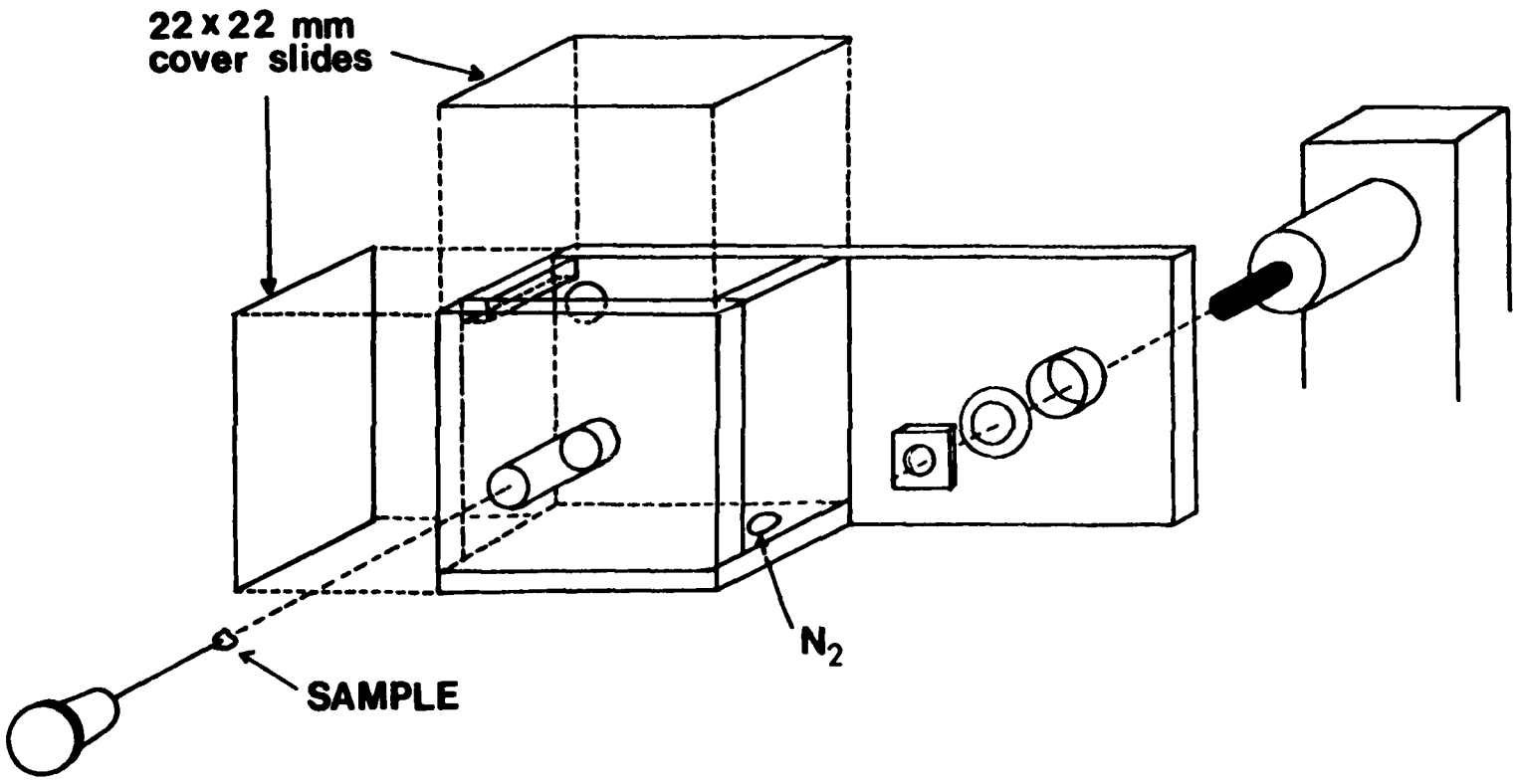
22 x 22 mm
cover slides
N_2
SAMPLE

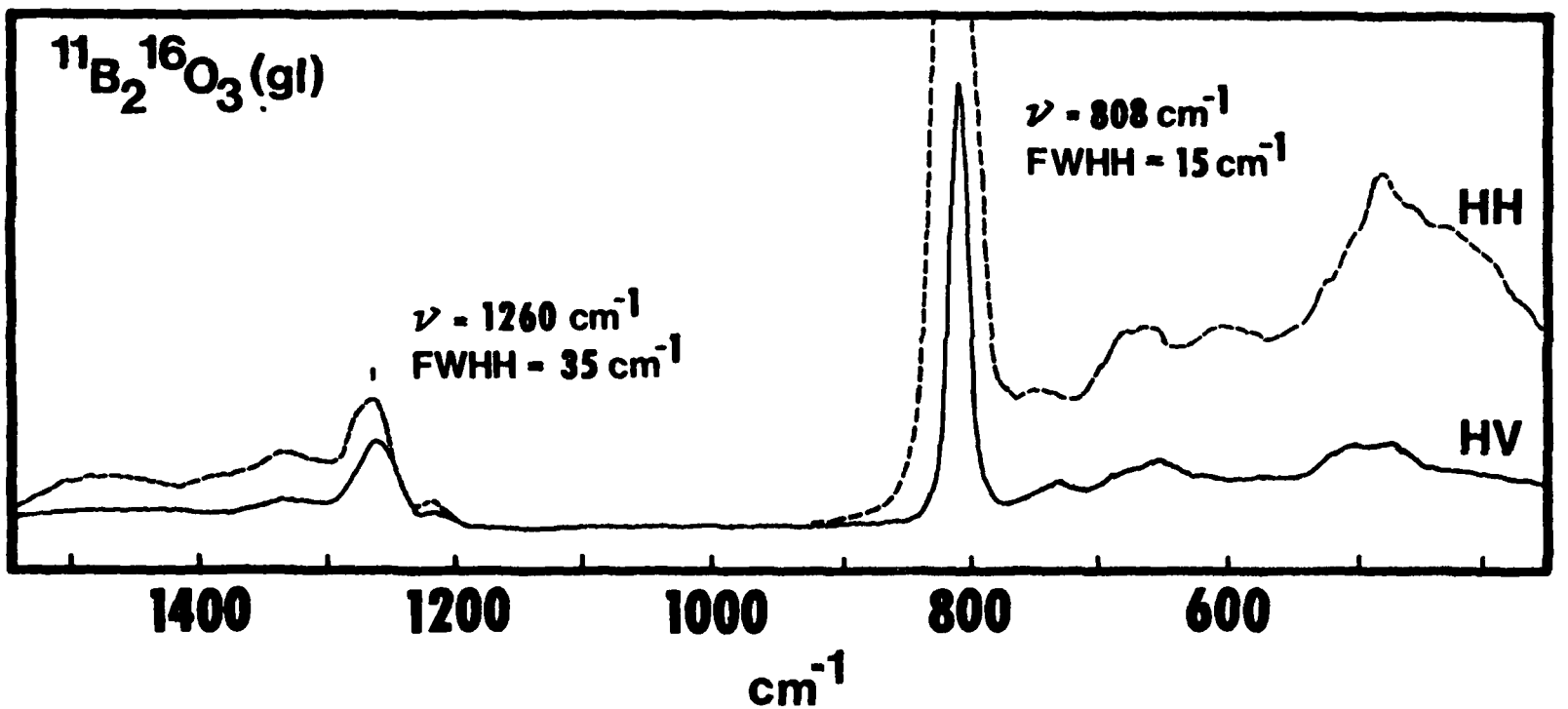
$^{11}B_2{}^{16}O_3$(gl)
ν = 808 cm^{-1}
FWHH = 15 cm^{-1}
HH
ν = 1260 cm^{-1}
FWHH = 35 cm^{-1}
HV
1400
1200
1000
800
600
cm^{-1}

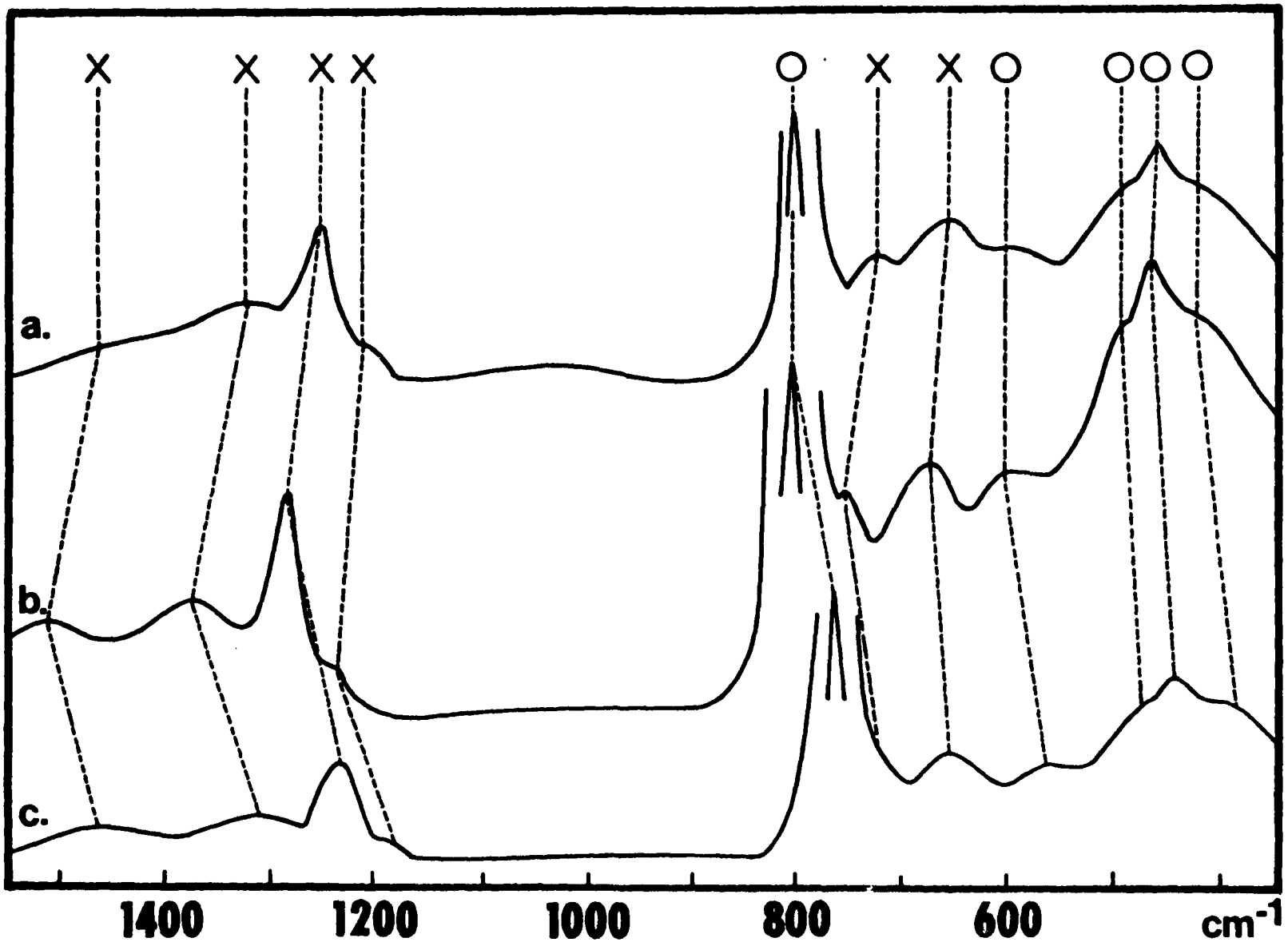
a.
b.
c.
1400
1200
1000
800
600
cm-1

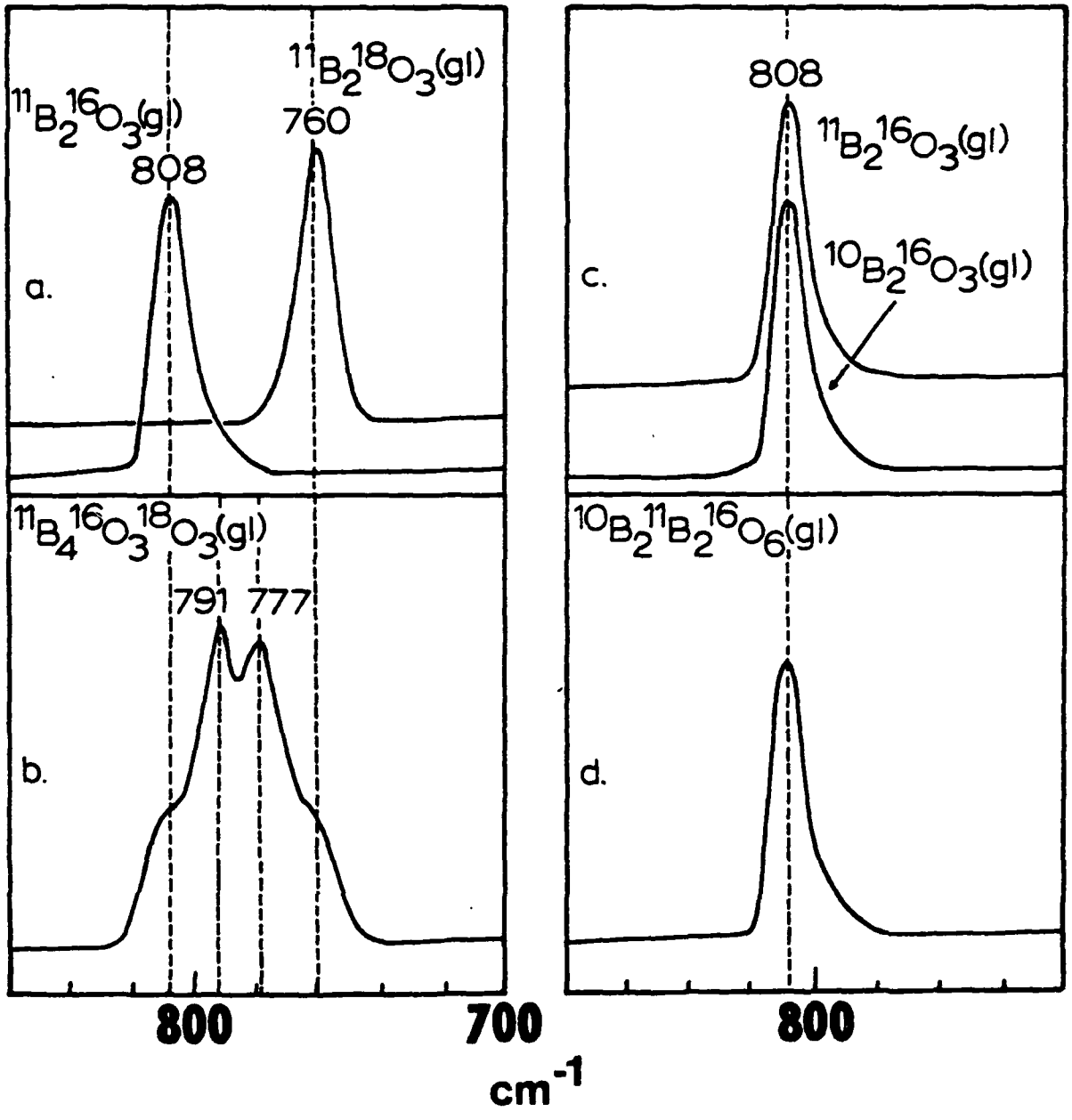
$^{11}B_2{}^{16}O_3$(gl)
808
$^{11}B_2{}^{18}O_3$(gl)
760
a.
$^{11}B_4{}^{16}O_3{}^{18}O_3$(gl)
791
777
b.
808
$^{11}B_2{}^{16}O_3$(gl)
$^{10}B_2{}^{16}O_3$(gl)
c.
$^{10}B_2{}^{11}B_2{}^{16}O_6$(gl)
d.
800
700
800
cm^{-1}

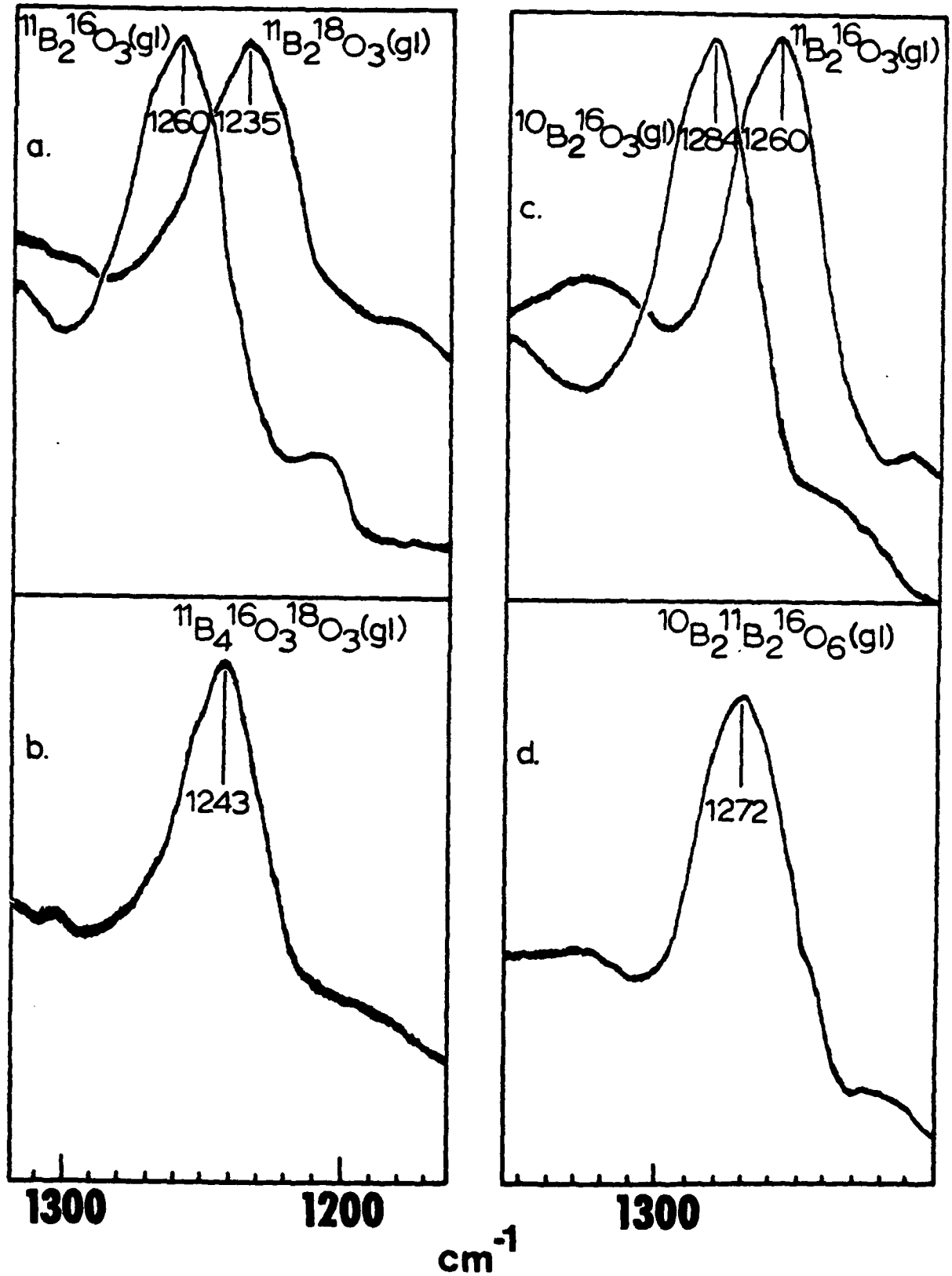
$^{11}B_2{}^{16}O_3$(gl)
$^{11}B_2{}^{18}O_3$(gl)
1260
1235
a.
$^{11}B_4{}^{16}O_3{}^{18}O_3$(gl)
b.
1243
$^{10}B_2{}^{16}O_3$(gl)
1284
1260
$^{11}B_2{}^{16}O_3$(gl)
c.
$^{10}B_2{}^{11}B_2{}^{16}O_6$(gl)
d.
1272
1300
1200
1300
cm^{-1}

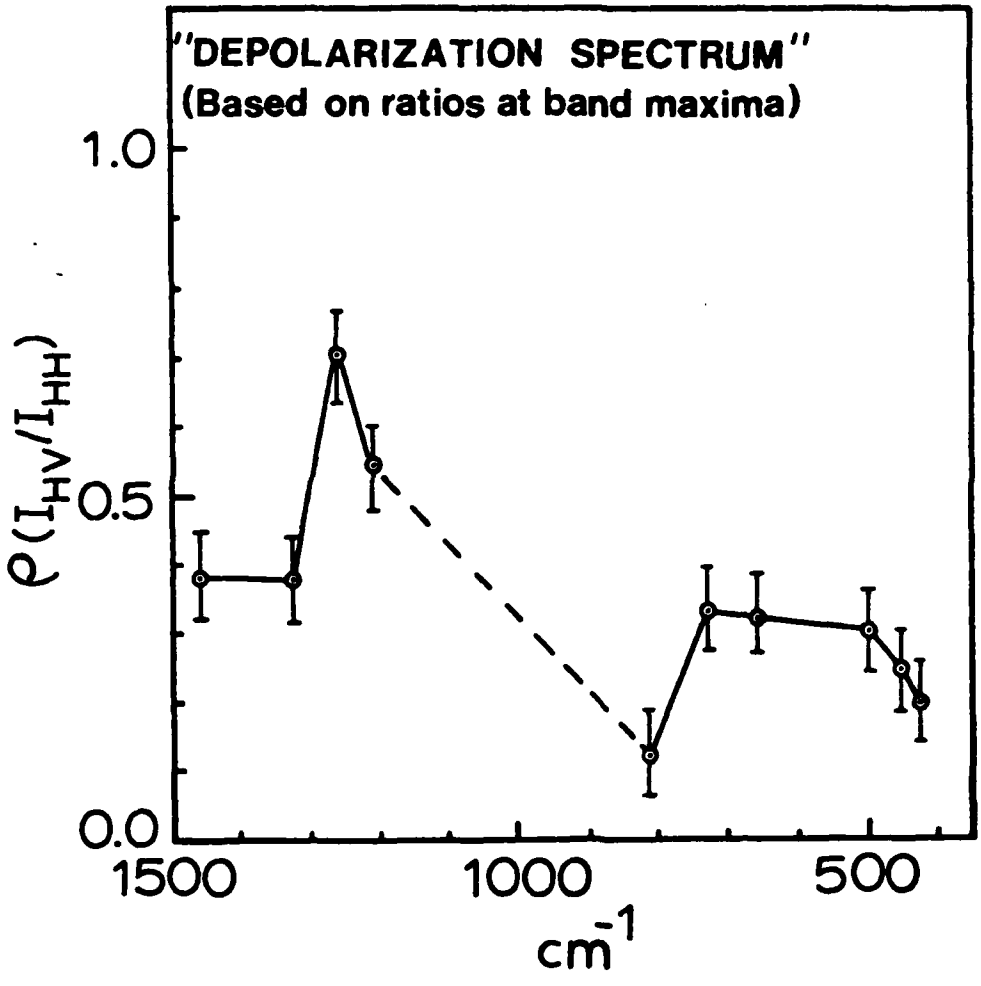
"DEPOLARIZATION SPECTRUM"
(Based on ratios at band maxima)
1.0
0.5
0.0
$\rho(I_{HV}/I_{HH})$
1500
1000
500
cm^{-1}

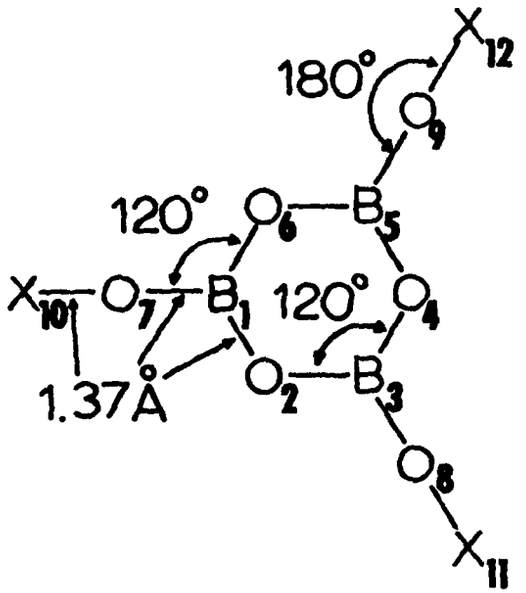
180°
X12
O9
120°
O6
B5
X10
O7
B1
120°
O4
1.37Å
O2
B3
O8
X11

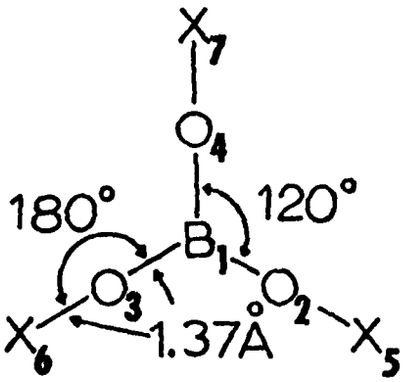
X7
O4
180°
120°
B1
O3
O2
X6
1.37Å
X5

TOTALLY SYMMETRIC MODES

Boroxol	Boroxol (isol.)	BO_3X_3
ν_1=1503 cm^{-1} 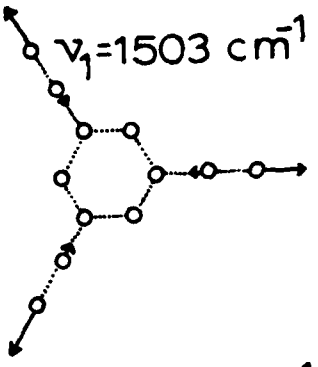		ν_1=1508 cm^{-1} 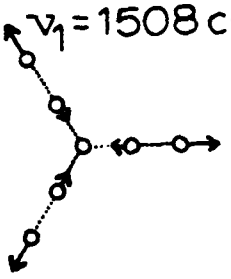
ν_2=1283 cm^{-1} 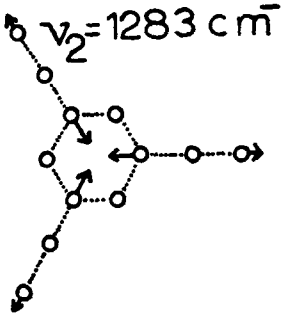	ν_1=1318 cm^{-1} 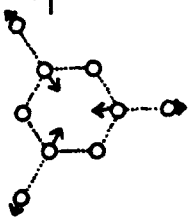	ν_2=697 cm^{-1} 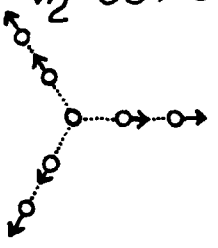
ν_3=808 cm^{-1} 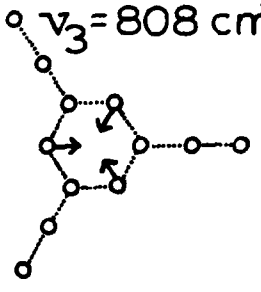	ν_2=808 cm^{-1} 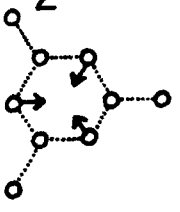	
ν_4=490 cm^{-1} 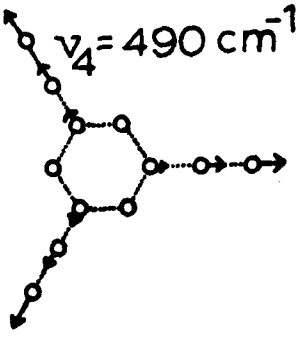	ν_3=554 cm^{-1} 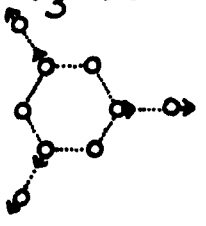	

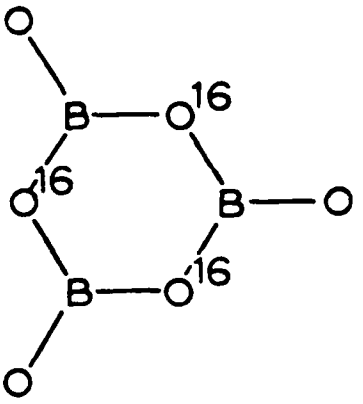

ν_3(obs.) = 808 cm^{-1}

ν_3(calc.) = 808 cm^{-1}

Rel. Comp. = 0.125

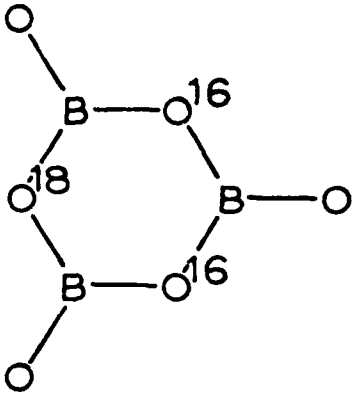

ν_3(obs.) = 791 cm^{-1}

ν_3(calc.) = 793 cm^{-1}

Rel. Comp. = 0.375

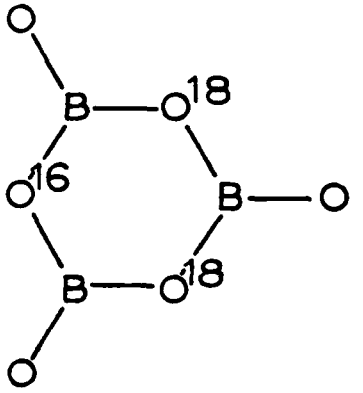

ν_3(obs.) = 777 cm^{-1}

ν_3(calc.) = 777 cm^{-1}

Rel. Comp. = 0.375

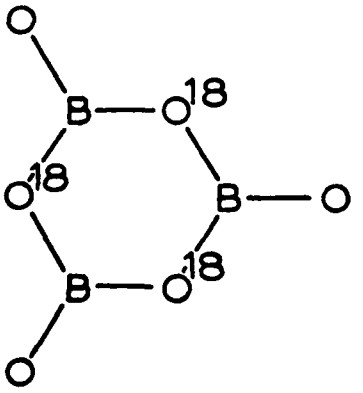

ν_3(obs.) = 760 cm^{-1}

ν_3(calc.) = 762 cm^{-1}

Rel. Comp. = 0.125

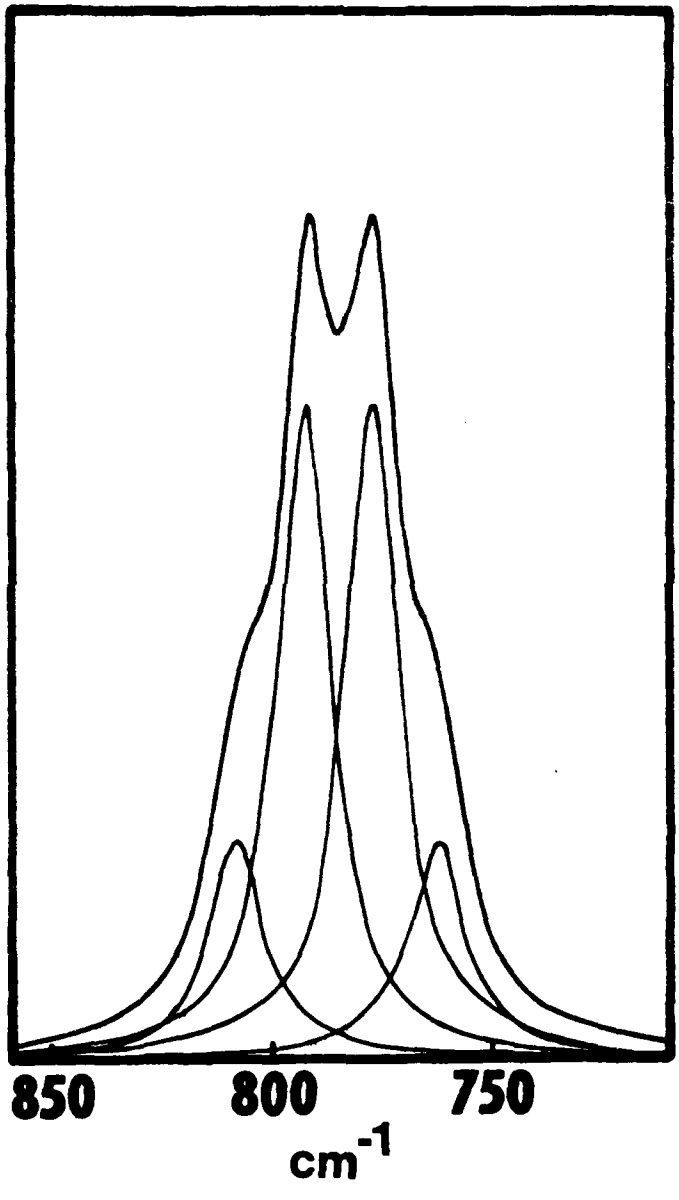
850
800
750
cm-1

SP472-3/A1

472:GAN:716:enj
78u472-608

TECHNICAL REPORT DISTRIBUTION LIST, GEN

	No. Copies
Office of Naval Research Attn: Code 472 800 North Quincy Street Arlington, Virginia 22217	2
ONR Western Regional Office Attn: Dr. R. J. Marcus 1030 East Green Stree Pasadena, California 91106	1
ONR Eastern Regional Office Attn: Dr. L. H. Peebles Building 114, Section D 666 Summer Street Boston, Massachusetts 02210	1
Director, Naval Research Laboratory Attn: Code 6100 Washington, D.C. 20390	1
The Assistant Secretary of the Navy (RE&S) Department of the Navy Room 4E736, Pentagon Washington, D.C. 20350	1
Commander, Naval Air Systems Command Attn: Code 310C (H. Rosenwasser) Department of the Navy Washington, D.C. 20360	1
Defense Technical Information Center Building 5, Cameron Station Alexandria, Virginia 22314	12
Dr. Fred Saalfeld Chemistry Division, Code 6100 Naval Research Laboratory Washington, D.C. 20375	1
U.S. Army Research Office Attn: CRD-AA-IP P.O. Box 1211 Research Triangle Park, N.C. 27709	1
Naval Ocean Systems Center Attn: Mr. Joe McCartney San Diego, California 92152	1
Naval Weapons Center Attn: Dr. A. B. Amster, Chemistry Division China Lake, California 93555	1
Naval Civil Engineering Laboratory Attn: Dr. R. W. Drisko Port Hueneme, California 93401	1
Department of Physics & Chemistry Naval Postgraduate School Monterey, California 93940	1
Scientific Advisor Commandant of the Marine Corps (Code RD-1) Washington, D.C. 20380	1
Naval Ship Research and Development Center Attn: Dr. G. Bosmajian, Applied Chemistry Division Annapolis, Maryland 21401	1
Naval Ocean Systems Center Attn: Dr. S. Yamamoto, Marine Sciences Division San Diego, California 91232	1
Mr. John Boyle Materials Branch Naval Ship Engineering Center Philadelphia, Pennsylvania 19112	1

TECHNICAL REPORT DISTRIBUTION LIST, GEN

	No. Copies
Mr. James Kelley DTNSRDC Code 2803 Annapolis, Maryland 21402	1
Mr. A. M. Anzalone Administrative Librarian PLASTEC/ARRADCOM Bldg 3401 Dover, New Jersey 07801	1

SP472-3/35

472:GAN:716:enj
78u472-608

TECHNICAL REPORT DISTRIBUTION LIST, 356A

	No. Copies
Dr. Stephen H. Carr Department of Materials Science Northwestern University Evanston, Illinois 60201	1
Dr. M. Broadhurst Bulk Properties Section National Bureau of Standards U.S. Department of Commerce Washington, D.C. 20234	2
Professor G. Whitesides Department of Chemistry Massachusetts Institute of Technology Cambridge, Massachusetts 02139	
Dr. D. R. Uhlmann Department of Metallurgy and Material Science Massachusetts Institute of Technology Cambridge, Massachusetts 02139	1
Naval Surface Weapons Center Attn: Dr. J. M. Augl, Dr. B. Hartman White Oak Silver Spring, Maryland 20910	1
Dr. G. Goodman Globe Union Incorporated 5757 North Green Bay Avenue Milwaukee, Wisconsin 53201	1
Professor Hatsuo Ishida Department of Macromolecular Science Case-Western Reserve University Cleveland, Ohio 44106	1
Dr. David Soong Department of Chemical Engineering University of California Berkeley, California 94720	
Dr. Curtis W. Frank Department of Chemical Engineering Stanford University Stanford, California 94305	
Picatinny Arsenal Attn: A. M. Anzalone, Building 3401 SMUPA-FR-M-D Dover, New Jersey 07801	1
Dr. J. K. Gillham Department of Chemistry Princeton University Princeton, New Jersey 08540	1
Dr. E. Baer Department of Macromolecular Science Case Western Reserve University Cleveland, Ohio 44106	1
Dr. K. D. Pae Department of Mechanics and Materials Science Rutgers University New Brunswick, New Jersey 08903	1
NASA-Lewis Research Center Attn: Dr. T. T. Serofini, MS-49-1 21000 Brookpark Road Cleveland, Ohio 44135	1
Dr. Charles H. Sherman Code TD 121 Naval Underwater Systems Center New London, Connecticut 06320	1
Dr. William Risen Department of Chemistry Brown University Providence, Rhode Island 02192	1
Dr. Alan Gent Department of Physics University of Akron Akron, Ohio 44304	1
Mr. Robert W. Jones Advanced Projects Manager Hughes Aircraft Company Mail Station D 132 Culver City, California 90230	1

TECHNICAL REPORT DISTRIBUTION LIST, 356A

	No. Copies
Dr. C. Giori IIT Research Institute 10 West 35 Street Chicago, Illinois 60616	1
Dr. R. S. Roe Department of of Materials Science and Metallurgical Engineering University of Cincinnati Cincinnati, Ohio 45221	1
Dr. Robert E. Cohen Chemical Engineering Department Massachusetts Institute of Technology Cambridge, Massachusetts 02139	1
Dr. T. P. Conlon, Jr., Code 3622 Sandia Laboratories Sandia Corporation Albuquerque, New Mexico	1
Dr. Martin Kaufmann, Head Materials Research Branch, Code 4542 Naval Weapons Center China Lake, California 93555	1
Professor S. Senturia Department of Electrical Engineering Massachusetts Institute of Technology Cambridge, Massachusetts 02139	1
Dr. T. J. Reinhart, Jr., Chief Composite and Fibrous Materials Branch Nonmetallic Materials Division Department of the Air Force Air Force Materials Laboratory (AFSC) Wright-Patterson AFB, Ohio 45433	1
Dr. J. Lando Department of Macromolecular Science Case Western Reserve University Cleveland, Ohio 44106	1
Dr. J. White Chemical and Metallurgical Engineering University of Tennessee Knoxville, Tennessee 37916	1
Dr. J. A. Manson Materials Research Center Lehigh University Bethlehem, Pennsylvania 18015	1
Dr. R. F. Helmreich Contract RD&E Dow Chemical Co. Midland, Michigan 48640	1
Dr. R. S. Porter Department of Polymer Science and Engineering University of Massachusetts Amherst, Massachusetts 01002	1
Professor Garth Wilkes Department of Chemical Engineering Virginia Polytechnic Institute and State University Blacksburg, Virginia 24061	1
Dr. Kurt Baum Fluorochem Inc. 680 S. Ayon Avenue Azuza, California 91702	1
Professor C. S. Paik Sung Department of Materials Sciences and Engineering Room 8-109 Massachusetts Institute of Technology Cambridge, Massachusetts 02139	1
Professor Brian Newman Department of Mechanics and Materials Science Rutgers, The State University Piscataway, New Jersey 08854	1
Dr. John Lundberg School of Textile Engineering Georgia Institute of Technology Atlanta, Georgia 30332	1

END

DATE

FILMED